PROCEEDINGS OF SPIE

SPIEDigitalLibrary.org/conference-proceedings-of-spie

A holistic metrology sensitivity study for pattern roughness quantification on EUV patterned device structures with mask design induced roughness

Shimon Levi, Ishai Swrtsband, Vladislav Kaplan, Ilan Englard, Kurt Ronse, et al.

Shimon Levi, Ishai Swrtsband, Vladislav Kaplan, Ilan Englard, Kurt Ronse, Bogumila Kutrzeba-Kotowska , Gaoliang Dai, Frank Scholze, Kenslea Anne, Hayley Johanesen, Laurens Kwakman, Igor Turovets, Maxim Rabinovitch, Sven Krannich, Nikolai Kasper, Brid Connolly, Romy Wende, Markus Bender, "A holistic metrology sensitivity study for pattern roughness quantification on EUV patterned device structures with mask design induced roughness," Proc. SPIE 10585, Metrology, Inspection, and Process Control for Microlithography XXXII, 1058511 (2 August 2018); doi: 10.1117/12.2297265

SPIE.

Event: SPIE Advanced Lithography, 2018, San Jose, California, United States

A holistic metrology sensitivity study for pattern roughness quantification on EUV Patterned device structures with mask design induced roughness

Shimon Levi[a], Ishai Swrtsband[a], Vladislav Kaplan[a], Ilan Englard[a], Kurt Ronse[b], Bogumila Kutrzeba-Kotowska[b], Gaoliang Dai[c], Frank Scholze[c], Anne Kenslea[d], Hayley Johanesen [d], Laurens Kwakman[d], Igor Turovets[e], Maxim Rabinovitch[e], Sven Krannich[f], Nikolai Kasper[f], Brid Connolly[g], Romy Wende[g], Markus Bender[h]

a APPLIED MATERIALS, 9 Oppenheimer St., Rehovot 76705, Israel
b Imec, Kapeldreef 75, 3001 Leuven, Belgium
c Physikalisch-Technische Bundesanstalt, Bundesallee 100, 38116 Braunschweig, Germany
d FEI, Achtseweg Noord 5, 5651 GG Eindhoven, The Netherlands
e NOVA, Weizmann Science Park, Rehovot 7610201, Israel
f BRUKER JV, Ramat Gavriel Industrial Zone Migdal Ha'Emek 23100, Israel
g TOPPAN PHOTOMASKS Germany GMBH , Rähnitzer Allee 9, 01109 Dresden, Germany
h AMTC, Rähnitzer Allee 9, 01109 Dresden, Germany

ABSTRACT

Monitoring of pattern roughness for advanced technology nodes is crucial as this roughness can adversely affect device yield and degrade device performance. The main industry work horse for in-line roughness measurements is the CD-SEM, however, today no adequate reference metrology tools exist that allow to evaluate its roughness measurement sensitivity and precision. To bridge this gap, in this work the roughness measurement capabilities of different analytical techniques are investigated. Different metrology methods are used to evaluate roughness on a same set of samples and results are compared and used in a holistic approach to better characterize and quantify the measured pattern roughness. To facilitate the correlation between the various metrology techniques and the evaluation of CD-SEM sensitivity, an effective approach is to induce pattern roughness in a controlled way by adding well defined levels of roughness to the designed patterns on a EUV mask and to measure the response and sensitivity of CD-SEM and of the other techniques to these different pattern roughness levels once printed on wafers. This paper presents the roughness measurement results obtained with various metrology technologies including CD-SEM, OCD, S-TEM and XCD on EUV Lithography patterned wafers both post-lithography and post-etch. The benefits of recently developed metrology enhancements are demonstrated as well; automated TEM allows to generate accurate and rather precise reference roughness data, Machine Learning enables OCD based roughness metrology with good correlation to CD-SEM and STEM, and the improved sensitivity of EUV and X-ray scattering systems allows to extract roughness information that does correlate to CD-SEM.

Keywords: Pattern roughness, holistic metrology, EUV scattering, X-ray scattering, OCD, STEM, CD-SEM, metrology precision, metrology sensitivity.

1. INTRODUCTION

Due to the small physical dimensions of integrated circuit structures, pattern roughness characterization, i.e. the detection of small random excursions from the mean geometrical parameters, poses a significant metrology challenge. Particularly, the measurement process may even change the structure geometry, e.g. the well-known electron beam induced resist-shrinkage or carbon deposition during SEM and TEM measurements. There are, however, many more like 'optical bleaching' in OCD or tip wear effects in AFM metrology. These various metrology specific effects add to measurement uncertainty and, therefore, a single measurement cannot provide unambiguous results.

Metrology, Inspection, and Process Control for Microlithography XXXII, edited by Vladimir A. Ukraintsev, Ofer Adan, Proc. of SPIE Vol. 10585, 1058511

While CD-SEM is used on a routine basis for pattern roughness monitoring, adequate reference metrology is lacking to verify its measurement sensitivity and uncertainty. Traditional TEM microscopy has the ultimate resolution to measure structural variations locally at the sub-nm scale, but TEM is considered too slow for generating any statistically relevant data. However, recent advances in the development of automated TEM metrology workflows open new ways to do statistically significant TEM analysis of line roughness in latest generation device structures. Other, more integrating and faster techniques such as X-ray scattering or optical scatterometry can detect the presence of line roughness in the recorded photon spectra, but the unknown sensitivity and the complex extraction of the line roughness information from the spectra make quantification a non-trivial task. To leverage strengths and weaknesses of the different metrology methods, combining and correlating CD-SEM, TEM, optical scatterometry and X-ray based roughness analysis results may help to better understand and to improve the capabilities of these roughness metrology techniques in terms of sensitivity, precision and efficiency.

Therefore, the purpose of this study is to evaluate the capabilities of these different in-line and off-line metrology techniques to measure roughness of different patterned structures, to compare the results obtained and to understand how these techniques can be combined to arrive at best roughness characterization methodologies. To explore pattern roughness measurement sensitivity and uncertainty of these metrology techniques in more details, test patterns were designed that incorporate induced roughness with defined spatial frequencies and amplitudes. A set of two EUV masks including these patterns was designed, fabricated and used to transfer these patterns onto wafers. The details of the sample structures and the experimental plan are described hereafter.

2. DESIGN OF EXPERIMENTS

A CAD layout was designed to form metrology targets with induced roughness on the EUV reticles, in sinusoidal and random, in-phase and out-of-phase arrangements with predefined (printed) wave lengths (30-720 nm) and amplitudes (0 - 6 nm). In table 1, the different targets that have been used in this study are listed. The EUV Masks were fabricated by Toppan, wafer patterning was done by imec on α-Silicon layer and on a more complex BEOL Metal 1 stack of layers (Fig. 1). Lithography was done in three different ways: at nominal exposure conditions (POR), at nominal focus and varying exposure dose conditions (EM) and at varying focus and exposure dose conditions (FEM). The hard mask and trench etch processes were done at nominal etch conditions (POR) but the trench etch was also done with varying etch times, to create trenches with varying depths and, potentially, different aspect ratios. Wafers were extracted and characterized after EUV litho resist patterning, Hard Mask etch and M1 dielectric trench etch process steps. To correlate the different metrology techniques, all wafers were measured by at least two or more metrology techniques: the α-Silicon wafers by two different X-ray and EUV scattering tools and CD-SEM, the M1 stack wafers after resist patterning by CD-SEM and OCD, after hard mask etch by CD-SEM, OCD and STEM and, finally, after dielectric trench etch by CD-SEM and STEM. Below the experimental results are presented for each of these metrology techniques.

Table 1. List of characterized BEOL targets (α-Silicon targets used by X-ray and EUV metrology tools are presented in table 2)

Target type (EUV mask 1)	Trench CD (nm)	Pitch (nm)	Induced Roughness	Wave Length (nm)	Amplitude (nm)
Natural Roughness	30	100	None	-	-
Chirped Sinusoidal	30	100	Off Phase	30-90	6
Random Roughness	30	100	Random	100 (*)	3
Natural Roughness	24	48	None	-	-

(*): correlation length

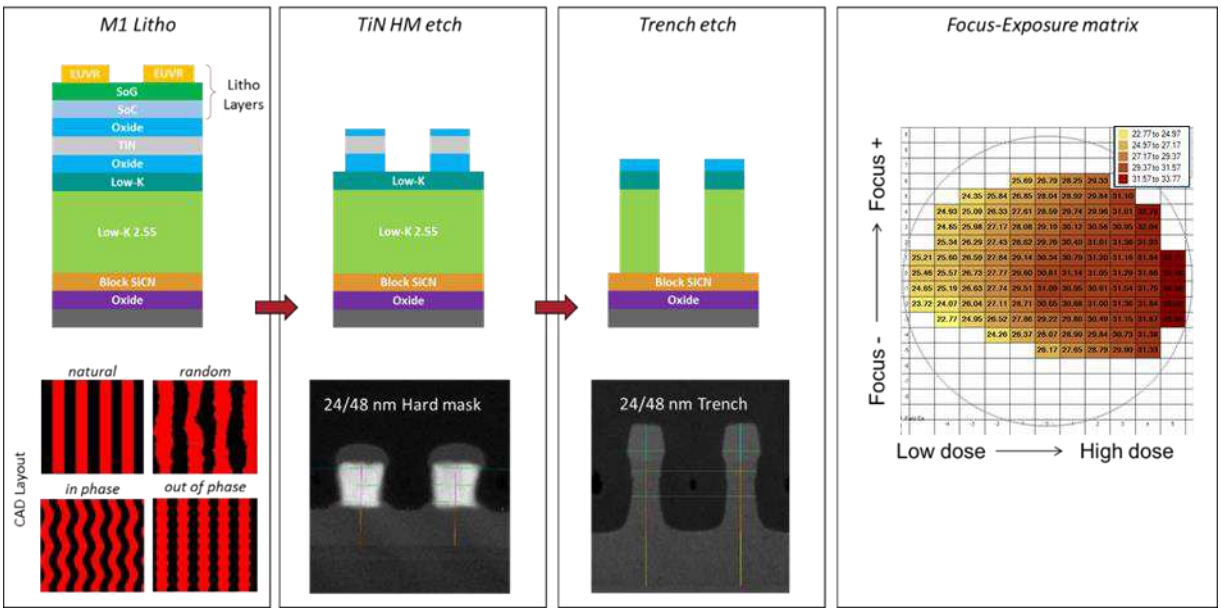

Figure 1. Imec's BEOL M1 patterning short loop wafers: three types of structures – Resist, TiN Hard Mask & Dielectric Trench- are analyzed by CD-SEM, OCD and STEM on FEM, EM and POR wafers fabricated for each.

3. CD-SEM METROLOGY

The CD-SEM algorithm is designed to sensitively detect pattern edges. Pattern edge data are generated in a form of topographical points, that are processed to calculate the pattern CD as well as the pattern roughness. A common approach to characterize roughness with CD-SEM is by transforming the 2D topographical points from the space domain into the frequency domain and using Power Spectral Density (PSD) analysis [1]. This approach enables to evaluate the dominance (power) of specific spatial frequencies or frequency bands in the measured pattern edges. The various targets listed in table 1 have been measured with CD-SEM after the different process steps and a PSD analysis was done. From this full PSD analysis, the roughness spread was integrated for three specified frequency bands, i.e. low frequency, LF < 1/200 nm, mid frequency , 1/200 < MF < 1/20 nm, and high frequency, HF > 1/ 20 nm. Roughness of low spatial frequency may indicate overlay or wiggling distortions whereas mid and high frequency bands can be related to the stoichiometry of materials, or deviation of different process steps and can impact electron/hole mobility or parasitic capacitance.

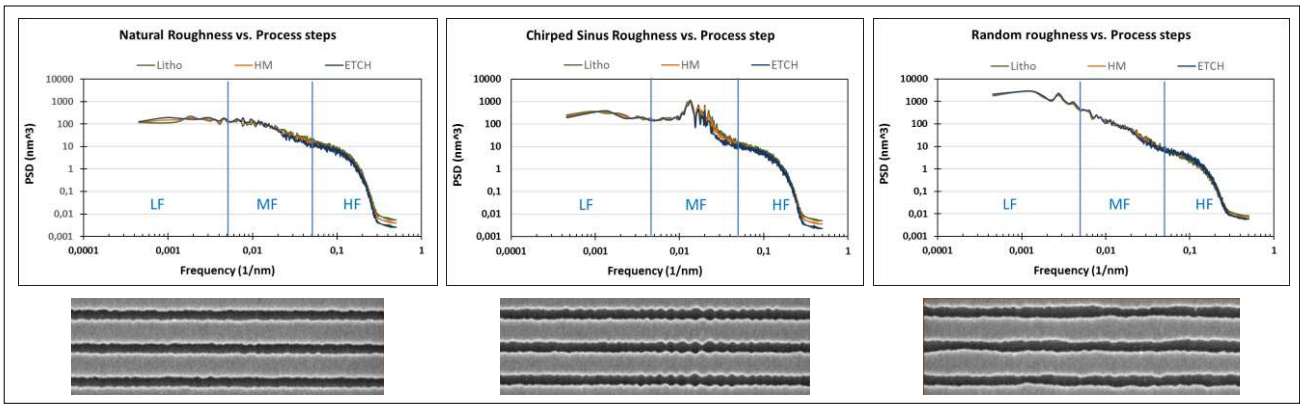

Figure2. PSD charts for three different targets measured at three different process steps (litho-HM etch-trench etch)

The PSD charts (Fig. 2) indicate that for this M1 process the pattern roughness characteristics are essentially the same for the line patterns after lithography, hard mask and trench etch process steps. It demonstrates that roughness is strongly defined by EUV lithography and transferred via etch steps to the final pattern edges. One can see distinguished peaks in the MF range of the chirped sinusoidal roughness target, these are well correlated with the out-of-phase sinus roughness induced on this pattern. The area underneath the PSD curves is the edge roughness calculated as 3 sigma deviations of topographical points from a straight line (LER) or as CD 3 sigma deviations from a rectangular line (LWR). Selecting three roughness bands enables to split LER or LWR roughness into 3 numbers, automatically measured by the tool and to use these numbers like CD measurements for process window characterization.

To evaluate how roughness is affected by focus and exposure settings, the targets were measured across a FEM wafer. Measurement results (Fig. 3 top) demonstrate that focus variations have the largest impact on EUV resist pattern roughness, especially in the MF range. When repeating the same measurements after hard mask and subsequent trench etch steps (Fig. 3 bottom), very similar results are obtained, again indicating that EUV lithography induced resist pattern roughness is transferred during the pattern transfer etch steps in the dielectric film pattern. For the HF range though, the wafer maps after litho and etch show a different center vs. periphery trend. Although the change is within the precision range of the CD-SEM, this clear trend is less likely to be formed by the CD-SEM tool and may be related to the etch process.

Interestingly, when comparing the effects of focus and exposure dose on line CD and roughness, different trends are observed (Fig. 4): whereas the effect of focus is most significant for roughness at mid frequency band, the opposite is true for the CD for which exposure dose has the largest impact. Characterizing roughness at different frequency bands provides additional perspective on each process step characteristics. Reflecting different cross wafer trends, CD and roughness need to be both measured to fully characterize the impact of these process settings on material characteristics, process window and ultimate device performance.

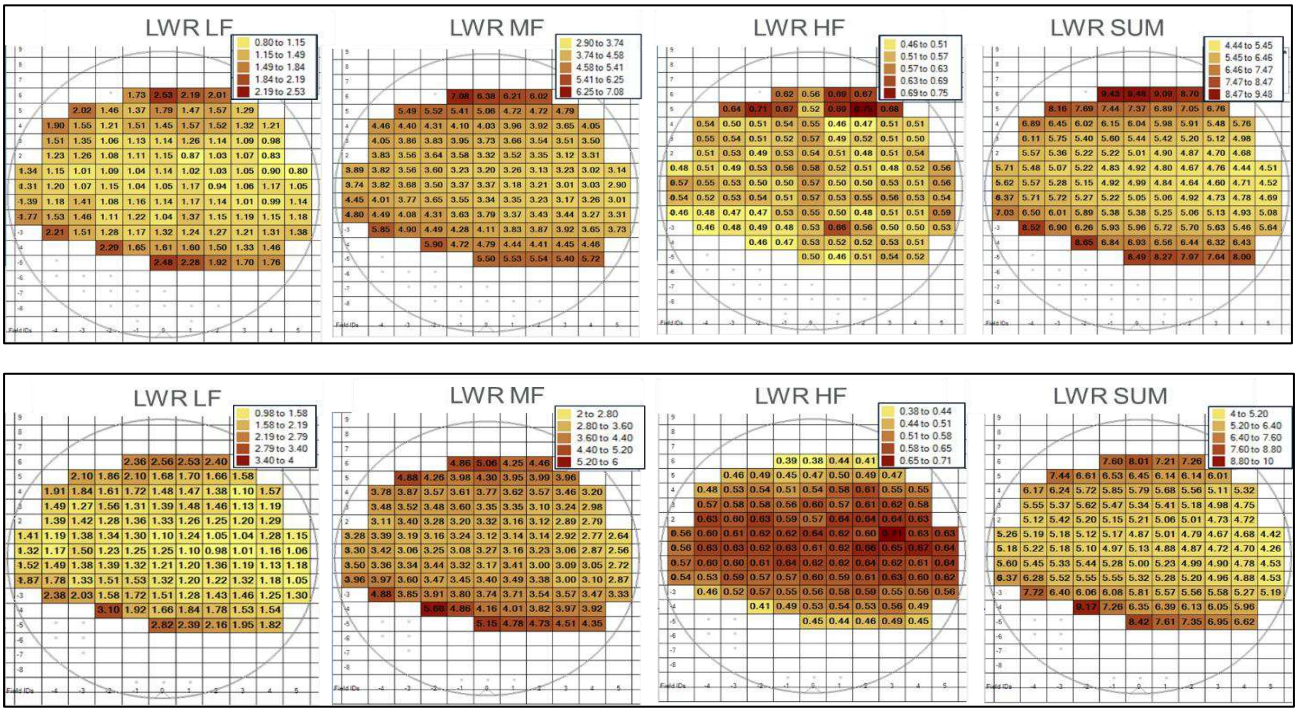

Figure 3. PSD analysis of a EUV-lithography FEM wafer, with roughness separated into low, mid and high frequency bands. Top row of wafer maps: roughness of the post-lithography EUV resist lines. Bottom row of wafer maps: roughness of the post-etch low-K dielectric lines.

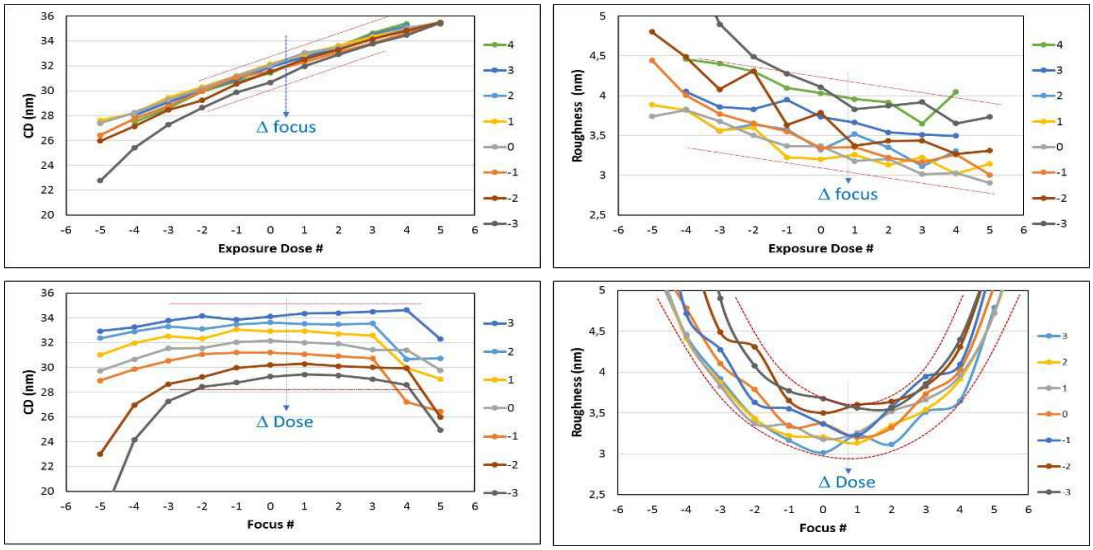

Figure 4. EUV process window characterization: CD and Roughness measure different trends. Roughness at MF, (lower right chart) suggests smaller process window vs CD.

Roughness measurement uncertainty was evaluated from reproducibility test runs using 10 consecutive measurements. After slope removal, results indicate a 3-sigma roughness measurement uncertainty of ~3% for EUV resist and ~2% for Etch. A CD-SEM noise suppression approach was applied to remove the noise added by the selected scan conditions and beam spot size.

To evaluate the sensitivity of the CD-SEM to specific types of pattern roughness, the correlation between LER and LWR measurements has been checked. LWR is commonly calculated using the following formula:

$$LWR^2 = (LER_{left})^2 + (LER_{right})^2 - 2 \times \text{Correlation function } (LER_{left}, LER_{right})$$

In case of stochastic roughness, no physical correlation is expected between the left and right edges, therefore the expected ratio between LWR and LER is $\sqrt{2}$. The LER vs. LWR graph (Fig. 5) for the target of natural roughness clearly reflects this ratio with a calculated slope of ~ 1.41 for all three spatial frequency ranges. When out-of-phase chirped sinusoidal roughness within a 0.01-0.03 nm^{-1} spatial frequency range is added to the natural pattern roughness, it is easily detected in the corresponding LWR vs. LER plot: the roughness data corresponding to the LF and HF ranges still fall on a line with slope ~1.41, but the data corresponding to the MF range that includes the added roughness show a shift towards higher roughness values and towards a higher LWR/LER ratio. Hence the results comply with the physical model and it demonstrates that PSD analysis in combination with LER/LWR correlation analysis can provide further insights, in the nature of the pattern roughness.

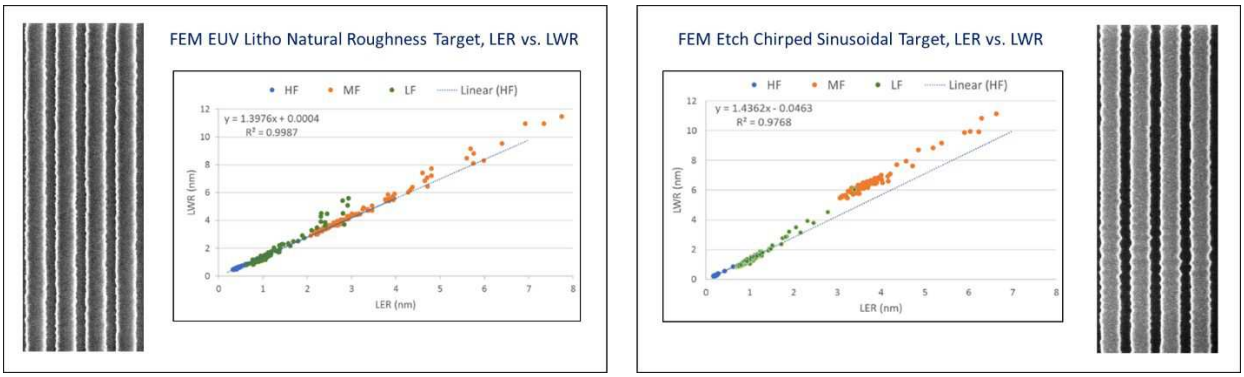

Figure 5. Correlations between LER and LWR for Litho FEM natural roughness (left) and for chirped sinusoidal roughness (right).

4. OCD AND CD-SEM ROUGHNESS CHARACTERIZATION

Optical scatterometry (OCD) is widely used in semiconductor manufacturing as in-line metrology technique: it is fast, non-destructive and has a proven capability to measure all details of complex 3D structures, including CDs, Side Wall Angles (SWA), heights, layer thicknesses, foot/notch, residues etc. One of the advantages of OCD for process control and monitoring is its capability to measure average values of parameters of interest on the measured target (on periodical structures or gratings) with unmatched precision and accuracy. Nevertheless, regular OCD was shown to be sensitive to the roughness (LER/LWR) of the features. In the paper by A. Vaid [2] it was shown, that measurements line profile (SWA) of 2D EUV photoresist (PR) lines by multi-angle spectral reflectometry was enabled only by accounting for the LER. In this paper LER was defined as an "effective spacer" covering the PR lines, and a CD-SEM hybridization scheme was proposed to accurately measure the profile of PR lines [2]. Similar observations were published recently by R. Bonam [3], where it was shown that for lines with the same CD but different build-in artificial roughness it is required to account for roughness to provide correct CD measurements. Direct influence of roughness on CD measurements was also shown in the work of Bilski [4] who proposed to use the CD differences measured at different polarizations as a measure of LER/LWR. Simulations were used in [5] to visualize the influence of roughness and to define best modeling and measurement conditions for roughness assessment by MMSE. Various models were used to describe "random" roughness by periodic structures that are required for rigorous OCD modelling, including "effective spacers", sinusoidal and rectangular variations of CD, with varying amplitude/frequency/correlation. Simulation results showed that in conical diffraction mode off-diagonal elements of the Mueller Matrix do provide information about Silicon Fin roughness. Also, limitations of the modelling of random effect of natural roughness with repetitive structure were clearly shown. In addition, the authors showed by simulations that measurements of natural roughness in EUV PR lines, with small CDs and heights will be more challenging for MMSE due to the reduced sensitivity.

In this study, multiple LER/LWR structures with natural and induced roughness have been measured after EUV litho and after low-K trench etch process steps with a Nova T600® MMSR (Multi Measurement Spectral Reflectometry) OCD system, that allows measurements at multiple azimuth angles with full control of polarization. Multiple wafers were measured, including FEM, EM, and trench depth DOE wafers described before. For all wafers, all dies were measured, with per die the 4 different target structures as listed in table 1, i.e. line patterns with just natural roughness and line patterns with mask induced roughness.

As already mentioned before, it has been found experimentally that both CD-SEM and OCD measurements can affect the sample structures: electron exposure in the CD-SEM causes resist and low-k dielectric shrinkage (in resist this effect is more pronounced), and UV radiation in the OCD system is modifying the optical properties of the materials. To decorrelate the effects of these physical phenomena in CD-SEM vs. OCD correlation studies, it was decided to not measure the same but identical structures at different locations in each field.

Machine learning (ML) algorithms based on CD-SEM measurement results were applied to train and optimize the OCD recipe for measuring and extracting the roughness parameters from the measured spectra. Here we present the results obtained with a ML based OCD recipe trained to measure CD and LWR of lines. Different approaches for ML recipe creation were used to check sensitivity to build–in roughness: we have created recipes per feature, and recipes for combination of features, and played with the reduction of the training sets by using different combination of features to test the recipes. For LWR measurements of similar Period/line CD features of 100/70 nm it was found that:

- Recipe trained for one of the features works best for the same feature, showing sensitivity to the build-in roughness components.
- Recipe trained at all features does not improve performance, compared with recipe per feature used for corresponding feature.

These observations show that there is sensitivity to build-in roughness, that is affecting different frequency domains. Additional work is required to create recipes that are capable to measure frequency components of LWR (LF, MF, HF).

OCD results are presented in Fig. 6 for CD and LWR measurements of resist (post-litho) and dielectric (post-trench etch) lines. Correlation to CD-SEM is good for all presented cases.

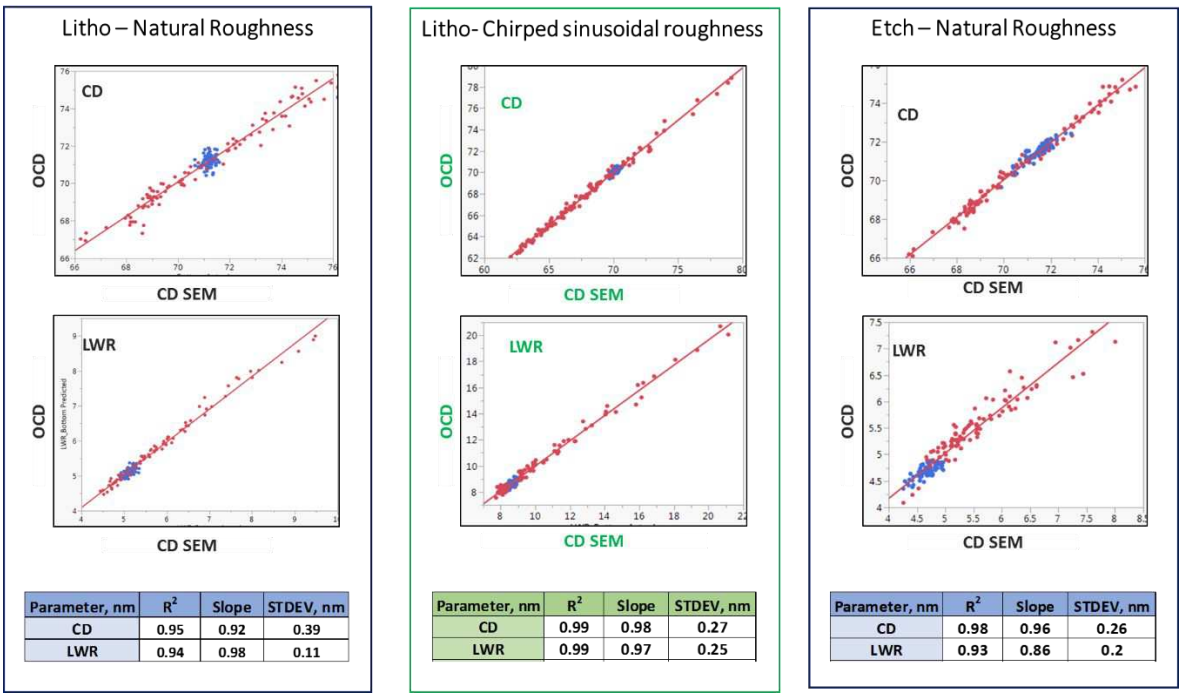

Parameter, nm	R^2	Slope	STDEV, nm
CD	0.95	0.92	0.39
LWR	0.94	0.98	0.11

Parameter, nm	R^2	Slope	STDEV, nm
CD	0.99	0.98	0.27
LWR	0.99	0.97	0.25

Parameter, nm	R^2	Slope	STDEV, nm
CD	0.98	0.96	0.26
LWR	0.93	0.86	0.2

Figure 6. Correlation between CD-SEM and OCD roughness measurements. CD and LWR measured by OCD with the ML algorithms. Left: post-litho EUV resist lines (70 nm, 100 nm pitch) with natural roughness. Middle: post-litho EUV resist lines (70 nm, 100 nm pitch) with added chirped sinusoidal roughness. Right: post-trench etch dielectric lines (70 nm, 100 nm pitch) with natural roughness. Blue and red datapoints correspond to measurements on POR and FEM wafers, respectively.

The wafer map data presented in Fig. 7 clearly show excellent matching of the OCD and CD-SEM LWR wafer maps for FEM wafers with large within wafer variations, while for POR wafers LWR map matching is less pronounced (average values and within wafer range matching is good). It is believed that larger training sets will improve the measurement accuracy of single measurements of LWR, which is supported by the observation that reduction of the current training sets (less dies, single wafer) leads to a performance degradation.

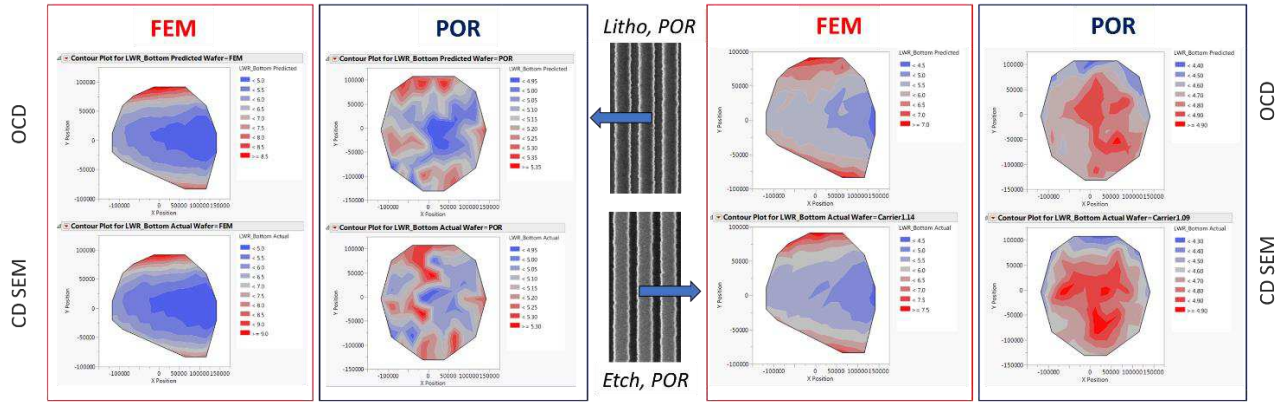

Figure 7. LWR wafer maps measured by CD-SEM and by OCD with ML algorithms. Left: post-litho EUV resist lines (70 nm, 100 nm pitch) with natural roughness measured on FEM and POR wafers. Right: post-trench etch dielectric lines (70 nm, 100 nm pitch) with natural roughness measured on FEM and POR wafers.

5. TRANSMISSION ELECTRON MICROSCOPY BASED ROUGHNESS CHARACTERIZATION

Recent developments in automation now enable metrology TEM systems to perform statistically significant TEM analysis of line roughness. The automation of the TEM workflow, including sample preparation, TEM image acquisition and image based metrology, brings TEM based metrology to a new level of efficiency and control [6]. The approach chosen here is illustrated in Fig. 8. Instead of making a top-down image of the line-space structure and measuring CDs across one line (the CD-SEM methodology), a lamella is extracted from the wafer and in this ~ 5 um wide lamella at least 60 lines and spaces (with pitch 48 nm) are contained. These lines are imaged in cross section and for each line and space the CD and pitch are measured. If it is assumed that the roughness is randomly distributed across one line and across multiple lines, the LWR can be calculated from the distribution of the individual line width CD measurements. As the cross-sectional STEM imaging method does not allow to determine the center of mass of each line it is not possible to determine the LER as is done with CD-SEM. However, the LER can be determined from the multiple pitch measurements. If no line edge roughness exists the distance between two adjacent line equals the nominal pitch (=48.00 nm for the selected test structures). However, with line edge roughness, each individual pitch measurement will have some variability:

$$\text{Pitch}_{ij} = \text{line} + \text{space} = \text{Pitch}_{nom} + \text{LER}_i \text{ (line1)} + \text{LER}_j \text{ (line2)} \quad (1)$$

$$\text{Var}(\text{Pitch}_{ij}) = \text{Var}(\text{LER}_i) + \text{Var}(\text{LER}_j) \quad \text{or} \quad 3\sigma_{\text{Pitch}} = \sqrt{2} \times \text{LER} \quad (2)$$

Hence, LER can be calculated from the distribution of individual pitch measurements.

The advantage of the STEM methodology is that apart from being able to generate quantitative numbers for both LWR and LER, it also allows to know exactly how the line profiles look like and to what exact part of the feature the LWR and LER relate to. In Fig. 8 this is illustrated in the middle image: the top and bottom images show different TiN lines in the same lamella. The variation in CD but also in Pitch is immediately seen in these images.

This STEM based methodology is applied first on the STEM metrology data obtained on 5 Trench etched wafers that each were etched with a different etch time. In Fig. 9 the STEM results are presented and compared to CD-SEM roughness data obtained on these same wafers and at identical Die locations. In the right image the dielectric lines are shown from wafers #03 and #21 that have shortest and longest etch times, respectively.

The correlation between CD-SEM and STEM roughness values has been further assessed on a post TiN Hard Mask wafer that because of the applied Focus-Exposure-Matrix has more process induced variation in line widths and in line roughness. The average TiN line width varies significantly as a function of exposure dose (see image in Fig. 10) but not as a function of focus setting. For the line roughness this trend is inversed, i.e. strongest variations in LER and LWR occur when the focus settings are varied.

From the data presented it is concluded that for both LER and LWR the STEM and CD-SEM measurements are in good agreement and both methods are able to detect the same process trend.

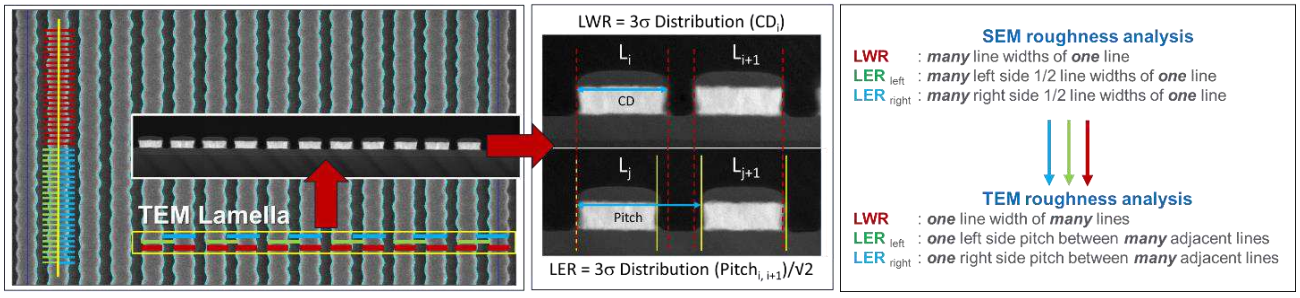

Figure 8. STEM based roughness analysis, the methodology.

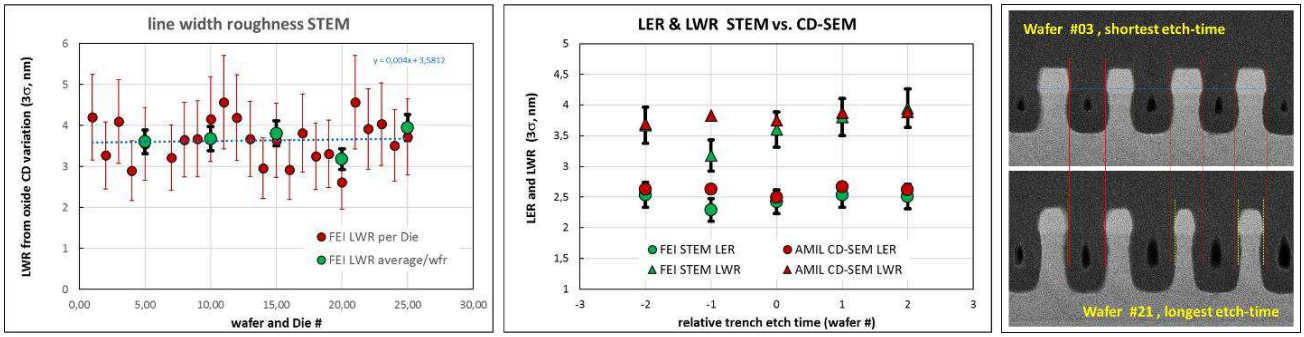

Figure 9. STEM and CD-SEM roughness measurements of trench etched wafers. Left: STEM LWR data from 5 wafers / 25 Die locations. Middle: correlation between STEM and CD-SEM roughness data. Right: STEM images of the analyzed structures. The error bars for the STEM data correspond with 95% confidence intervals, i.e. 2 standard errors.

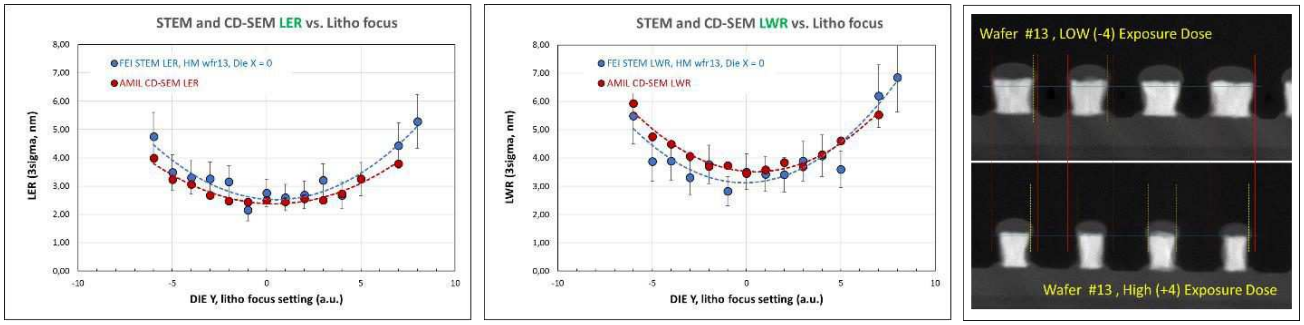

Figure 10. Correlation between STEM and CD-SEM Roughness measurement data for a Hard mask etched FEM wafer. LER and LWR data are plotted as a function of the focus setting at nominal exposure dose. Right: STEM images of the analyzed structures. The error bars for the STEM data correspond with 95% confidence intervals, i.e. 2 standard errors.

6. EUV VS. CD-SEM AND OCD SCATTERING ROUGHNESS CHARACTERIZATION

In an idealized figure, the X-ray or EUV scatter intensities of a periodic nanostructure can be described by the product of a so-called from factor and an interference factor. The interference factor is essentially the Fourier transform of the pattern periodicity and defines at which observation angles diffracted light can be observed. The form factor describes the geometry of the unit cell of the nanostructure array, e.g. the cross-section profile of a line. Roughness and imperfections of the periodic nanostructures lead to a smearing of the interference factor resulting in a reduction of the measured discrete diffraction intensities. This behavior (Debye-Waller damping initially observed in X-ray diffraction at the atomic crystal lattice) is generally known from X-ray scattering and was verified by the GISAXS measurements in the next section. Because the laboratory instruments used for EUV scattering are not particularly optimized for small targets on a wafer [7], we used special targets, listed in table 2, resembling a subset of the roughness designs used in the SEM, OCD and TEM studies, particularly also including chirped sinusoidal targets but with large dimensions (0.5 x 8 mm²) for the scattering measurements. The corresponding scatter distributions for the in-phase and out-of-phase chirped sinusoidal line roughness are shown in Fig. 11. The deterministic chirped structure induces an additional periodicity in the interference factor. In the scatter distribution this shows up as additional intensity spots aligned perpendicular to the diffraction spots of the basic grating structure. Only for in-phase line roughness (shown at the bottom of Figure 11), scatter satellites of the central specular (zero) diffraction order are observed (marked by the red rectangle in the figure). The modulation of the scatter intensity reveals the discrete frequency components of the chirped roughness profiles in the scatter field. The regular diffraction orders are the intense spots at the coordinate q_x=0. The red and green frames indicate the measurement area for the scatter radiation corresponding to about 700 nm spatial wavelength (lower bound) and 90 nm (upper bound). The right panel shows the

Table 2. list of X-ray scatter targets. *: for the random structures the characteristic wavelength is the roughness correlation length.

#	Target type (EUV mask 2)	Trench CD (nm)	Pitch (nm)	Induced Roughness	Wave Length (nm)	Amplitude (nm)
1	*Natural Roughness*	30	100	None	-	-
2	*Sinusoidal Roughness*	40	75	In- Phase	180	3
3	*Sinusoidal Roughness*	40	75	In- Phase	180	6
4	*Sinusoidal Roughness*	30	100	Out-of-phase	180	3
5	*Sinusoidal Roughness*	30	100	Out-of-phase	180	6
6	*Chirped Sinusoidal Roughness*	40	75	In- Phase	90 - 360	6
7	*Chirped Sinusoidal Roughness*	30	100	Out-of-phase	90-360	6
8	*Random Roughness*	30	100	random	50*	3
9	*Random Roughness*	30	100	random	200*	3
10	*Random Roughness*	30	100	random	50*	6
11	*Random Roughness*	30	100	random	200*	6
12	*Chirped Sinusoidal Roughness*	40	75	In-phase	30 - 90	6
13	*Chirped Sinusoidal Roughness*	30	100	Out-of-phase	30 - 90	6

intensity distribution of the roughness induced scatter as function of spatial wavelength for the 0th and 1st diffraction order. It should be noted that this distinction of in-phase against out-of-phase roughness via the 0th order satellite is unique for the EUV scattering measurements.

For comparability with GISAXS, where the scatter satellites are not directly measured, the Debye-Waller damping approach was used also to quantify the impact of the roughness in the EUV spectral range. The scattering intensities of all regular diffraction orders except the specular order are integrated for each of the different scattering targets. The right panel in Fig. 12 shows the total scattering intensity as a function of the roughness as measured with the CD-SEM. The data have a considerable variance which is caused by concurrent changes of CD and etch depth from structure to structure which also influence the diffraction intensities. A full modelling of the structures will resolve this issue. The measurements, however, demonstrate the potential and sensitivity of EUV scatterometry for the characterization of nanostructured surfaces. The type of line roughness can be easily identified in the scattering distribution. The amplitude of the line roughness can be determined by measuring the loss in diffraction efficiency. A sensitivity of 4.2 % loss/nm (LER 3σ) is demonstrated here for a wavelength of 11.3 nm. As compared to the GISAXS approach, EUV shows about the same sensitivity to roughness but the longer soft X-ray (EUV) wavelengths allow using steeper incidence angles, resulting in a smaller beam footprint on the sample. The steeper angle also results in a more isotropic angular distribution of the scatter, such that the scattered light corresponding to roughness wavelengths comparable to the structure pitch can directly be observed.

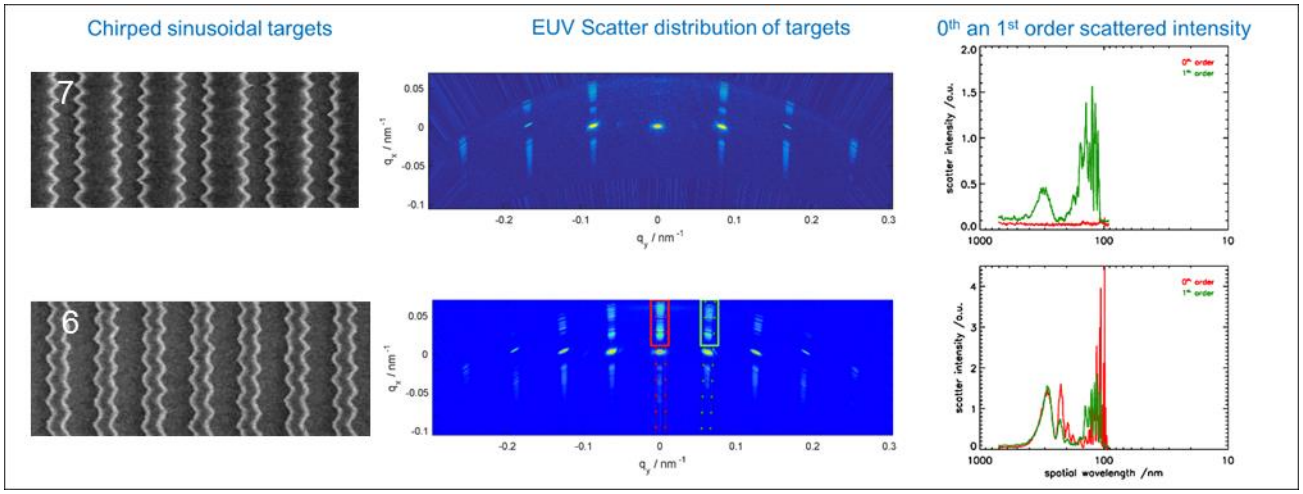

Figure 11. Top: SEM images and EUV scatter measurements in the center of the out-of-phase chirped scatter field; at the bottom CDSEM image and EUV scatter measurements in the center of the in-phase chirped scatter field.

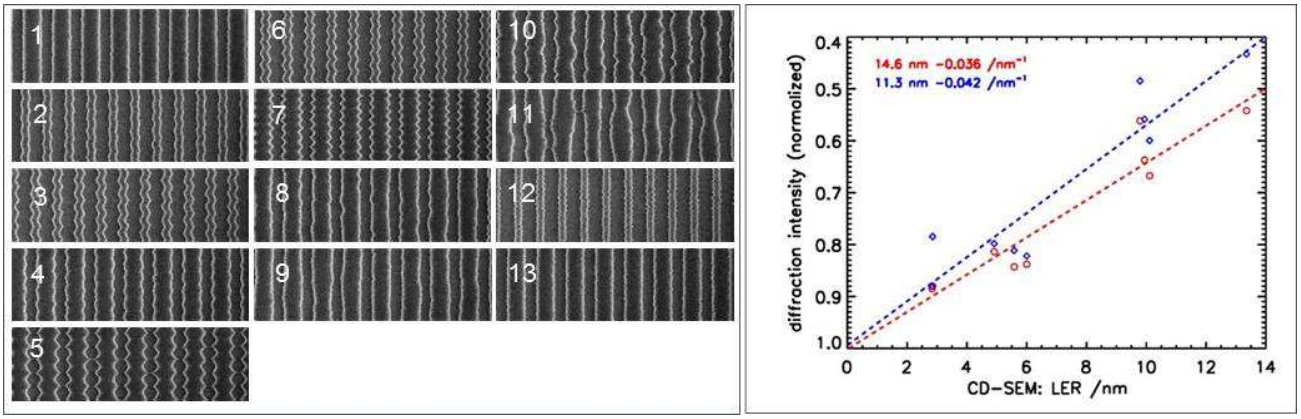

Figure 12. The EUV scattering experiments illustrated: left: CDSEM images of all 13 targets used for EUV / X-Ray analysis. Right: Integrated intensity of the main diffraction orders (excluding the specular order) as a function of the LER 3σ values measured by CD-SEM. Shown are data for two different wavelengths in the EUV spectral range for the structures with pitch 100 nm.

7. R-XCD VS. CD-SEM AND EUV ROUGHNESS CHARACTERIZATION

The same set of targets was measured by reflection-geometry-X-ray based CD (R-XCD) analysis. In R-XCD the intensity scattered from the surface of a periodically structured sample is measured.

The incident angle is kept close to the critical angle of total external reflection, i.e. <1°. From the intensity distribution of the X-ray scattering pattern measured using a high-resolution 2D pixel area detector, information on the lateral and vertical structural properties can be obtained through direct analysis and via refinement of the calculated intensity using a structural model of the sample. In X-ray scattering, roughness leads to a progressive damping of the scattered intensities with increase diffraction order. This signature can be found in the different scattering patterns as can be seen from the extracted line profiles in figure 13.

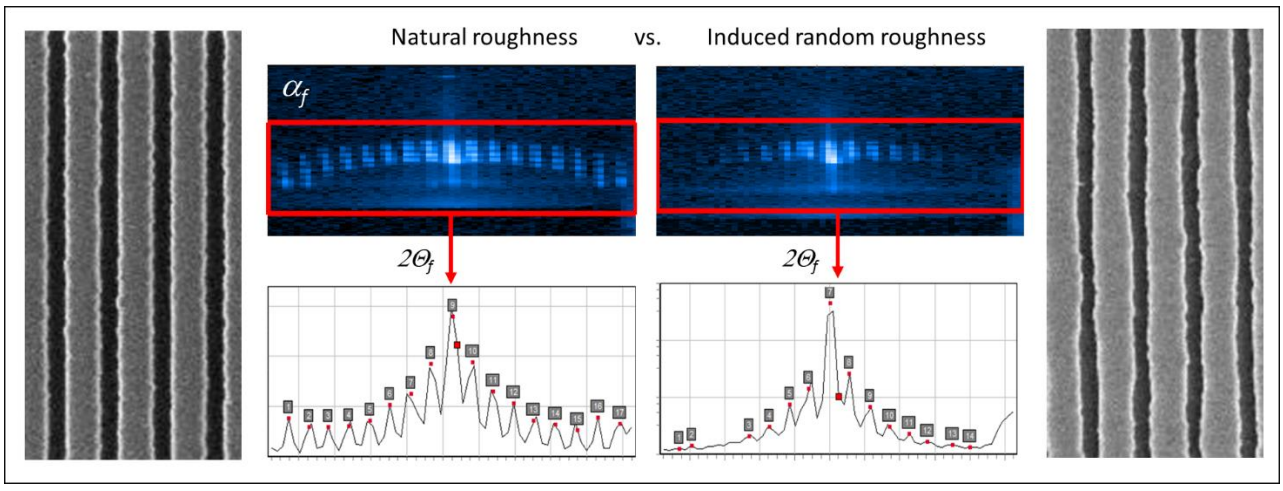

Figure 13. Representative R-XCD scattering patterns measured on a target with only process induced roughness (left) vs high amplitude sinusoidal roughness (right). The Truncation rod intensities have been extracted from the 2D image by integrating over α_f direction.

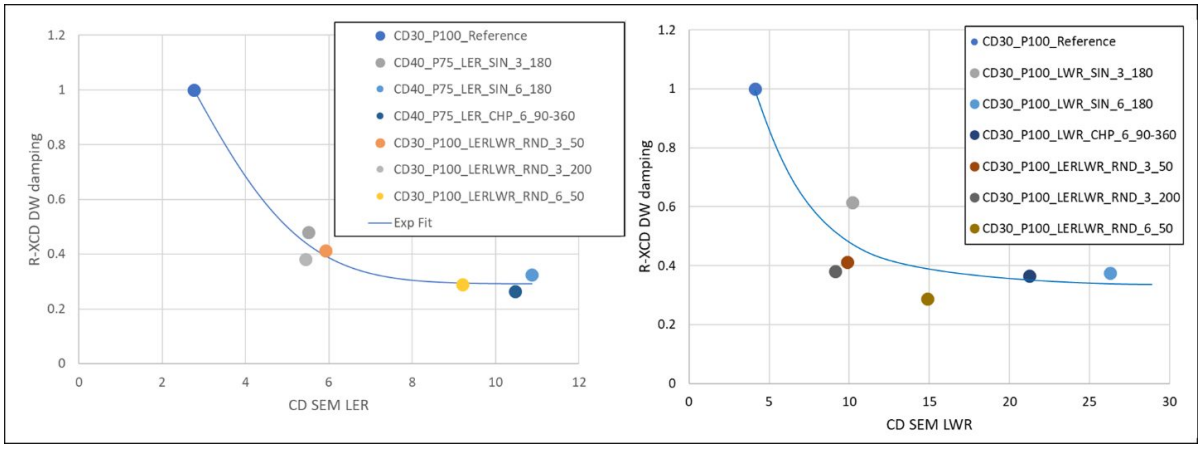

Figure 14. Correlation of the R-XCD damping vs. CD-SEM LER (left) and CD-SEM LWR (right), respectively.

To verify the sensitivity of our method, the scattered signal has further been analyzed and the data has been compared to LER and LWR results measured by CD-SEM. The graphs in Fig. 14 demonstrate the correlation between the R-XCD damping and the LER/LWR values obtained from CD-SEM measurements. The observed damping of scattered intensities in R-XCD follows an exponential decay of the form $I \sim \exp(-\sigma^2)$ with σ being the root-mean-square (RMS) roughness. The trend for LWR is very similar, but needs some further investigations, especially for the random roughness structures. In summary, it has been shown that R-XCD shows sensitivity to line roughness and results indicate a strong sensitivity especially at small amplitudes of the roughness.

8. CONCLUSIONS

The present studies have demonstrated that characterization and understanding of pattern roughness can be improved by using multiple metrology methods as correlation between these methods offers indications about measurement sensitivities and uncertainties, but also allows to evaluate roughness at different scales, i.e. from microscopic (single device structures over a ~ 5 µm length scale with CD-SEM, TEM) and mesoscopic (many device structures averaged over a ~ 50 µm length scale with OCD) to macroscopic (many device structures averaged over a ~ 5 mm length scale with EUV and X-ray scattering).

OCD sensitivity to pattern roughness has been demonstrated. By applying Machine Learning based on CD-SEM roughness datasets, the optical models can be optimized effectively to obtain OCD roughness data that match well with both CD-SEM and TEM roughness data. Especially for patterning process window studies where -due to focus and dose variations- roughness values show larger variations, OCD allows to do fast and reproducible roughness measurements, averaged over an array of device structures in a ~ 50x50 μm^2 area.

It is shown that STEM metrology can also be used for LER and LWR analysis and quantification. Thanks to the advanced levels of automation and control of state-of-the-art TEM microscopes, the lack of statistics is no longer a fundamental limitation of Transmission microscopy and relatively large STEM metrology datasets can now be generated within acceptable time frames. STEM and CD-SEM roughness data do correlate well, and STEM can be used as effective reference metrology to ensure that CD-SEM or OCD measurements are calibrated and relate to real physical roughness phenomena.

Also for EUV and R-XCD the sensitivity to LER and LWR has been demonstrated and results found in this study correlate well to CD-SEM measurements. This shows the potential of this technique for roughness measurements. However, a full quantification of CD and LER/LWR would require a full modelling which is the scope of future work.

Finally, the CD-SEM roughness and CD data for the various FEM wafers show that CD and roughness of the printed and etched structures can be uncorrelated. Therefore, in patterning process window studies both CD and roughness sensitivities are to be tested. PSD analysis is shown to be effective in determining how the process parameters (focus and dose) impact the nature of the roughness, i.e. spatial frequencies and amplitudes. Even for similar total roughness values, the predominant spatial frequencies can be different. This can be controlled by monitoring low, mid and high frequency bands.

ACKNOWLEDGEMENTS

This project has received funding from the Electronic Component systems for European Leadership Joint Undertaking under grant agreement No 621280. This Joint Undertaking receives support from the European Union's horizon 2020 research and innovation program at the Netherlands, France, Belgium, Germany, Czech Republic, Austria, Hungary, Israel.

REFERENCES

1. *Edge roughness characterization of advanced patterning processes using power spectral density analysis (PSD)* Shimon Levi et al, SPIE 9782, Advanced Etch Technology for Nanopatterning V, 97820I
2. *Hybrid metrology solution for 1X node technology*, A. Vaid et al, SPIE Adv. Litho. 2012
3. *An OCD perspective of line edge and line width roughness metrology*. R. Bonam et al, SPIE 10145, 2017
4. *Effective–CD: a contribution toward the consideration of line edge roughness in the scatterometric critical dimension metrology*, B. Bilski et al, J. Micro/Nanolith. MEMS MOEMS 16(2), 2017
5. *Sensitivity analysis and line edge roughness…. using optical critical dimension metrology*, D. Dixit et al, J. Micro/Nanolith. MEMS MOEMS 14(3), 2015
6. *Automated TEM workflows for Process Control*, O. Ugurlu, A. Kenslea, H. Johanesen, L. Kwakman, Proc. FCMN 2017
7. *EUV-angle resolved scatter (EUV-ARS): a new tool for the characterization of nanometre structures*, A. Fernández Herrero; H. Mentzel; V. Soltwisch; S. Jaroslawzew; C. Laubis; F. Scholze, Proc SPIE 10585, 105850P (2018)